

Direct NO decomposition over stepped transition-metal surfaces*

Hanne Falsig¹, Thomas Bligaard², Claus H. Christensen¹, and Jens K. Nørskov^{2,‡}

¹*Center for Sustainable and Green Chemistry, Department of Chemistry, Building 206, NanoDTU, Technical University of Denmark, DK-2800 Lyngby, Denmark;*

²*Center for Atomic-Scale Materials Design, Department of Physics, Building 311, NanoDTU, Technical University of Denmark, DK-2800 Lyngby, Denmark*

Abstract: We establish the full potential energy diagram for the direct NO decomposition reaction over stepped transition-metal surfaces by combining a database of adsorption energies on stepped metal surfaces with known Brønsted–Evans–Polanyi (BEP) relations for the activation barriers of dissociation of diatomic molecules over stepped transition- and noble-metal surfaces. The potential energy diagram directly points to why Pd and Pt are the best direct NO decomposition catalysts among the 3d, 4d, and 5d metals. We analyze the NO decomposition reaction in terms of a Sabatier–Gibbs-type analysis, and we demonstrate that this type of analysis yields results that to within a surprisingly small margin of error are directly proportional to the measured direct NO decomposition over Ru, Rh, Pt, Pd, Ag, and Au. We suggest that Pd, which is a better catalyst than Pt under the employed reaction conditions, is a better catalyst only because it binds O slightly weaker compared to N than the other metals in the study.

Keywords: NO; NO decomposition; Brønsted–Evans–Polanyi; activation barriers; dissociation; decomposition catalyst.

INTRODUCTION

Heterogeneous catalysis is one of the major industries worldwide. Catalysis is used to facilitate the production of many chemicals and materials that we use every day. It provides a range of products from fuels and fertilizers to plastics and pharmaceuticals. Catalysts are also utilized for the cleaning of exhaust from cars, power plants, and industrial production.

The proliferation of heterogeneous catalysis during the 20th century has indeed led to a significant improvement in the living standard of a large fraction of the world's population. It is perhaps therefore natural that one of the hundreds of important heterogeneous catalytic reactions was selected as the most important invention of the 20th century, ahead of the discovery of penicillin, the construction of the first transistor and the design of the integrated semiconductor circuit [1].

The increasingly stringent emission requirements for diesel engines require NO_x abatement technology, which is effective under lean-burn conditions. Various technologies such as NO_x traps [2] and

Pure Appl. Chem.* **79, 1831–2100. An issue of reviews and research papers based on lectures presented at the 1st International IUPAC Conference on Green–Sustainable Chemistry, held in Dresden, Germany, 10–15 September 2006.

‡Corresponding author

selective catalytic reduction (SCR) exist [3], but it would be preferable if a simpler process could be developed based on direct NO decomposition. In the direct NO decomposition reaction, the exhaust containing NO is flowed over a heterogeneously catalytic surface, where the NO bond is split, and N atoms recombine to N_2 while the O atoms recombine to O_2 . The direct NO decomposition reaction is thermodynamically favored at low temperatures, but it has proven difficult to find a catalyst that is both active and oxidation-resistant [4]. Here, we study the direct decomposition of NO over stepped transition-metal surfaces, since such step sites are known from theoretical calculations to be significantly more active for NO decomposition than the corresponding close-packed surfaces [5–9]. This enhanced reactivity of steps also explains why smaller transition-metal particles show enhanced activity for NO decomposition [10].

The way we normally perform such studies is by establishing a total energy diagram for each of the catalytic surfaces in question, as schematically shown in Fig. 1. The figure shows the energy levels for a catalytic reaction. The energies of transition-state structures and reaction intermediates on the surface are determined by employing density functional theory (DFT) in a plane wave/pseudopotential implementation. This methodology gives a very reasonable trade-off between accuracy and computational cost. The total energy diagrams are then analyzed in terms of harmonic transition-state theory to yield rates for individual elementary reactions, and these rates are then analyzed using microkinetic modeling to establish the overall catalytic rate per active site, the so-called turnover frequency. Often, it occurs that there is a correlation between the energies of transition-state structures corresponding to the activation of reactants and the key reaction intermediates (E_a and ΔE in Fig. 1).

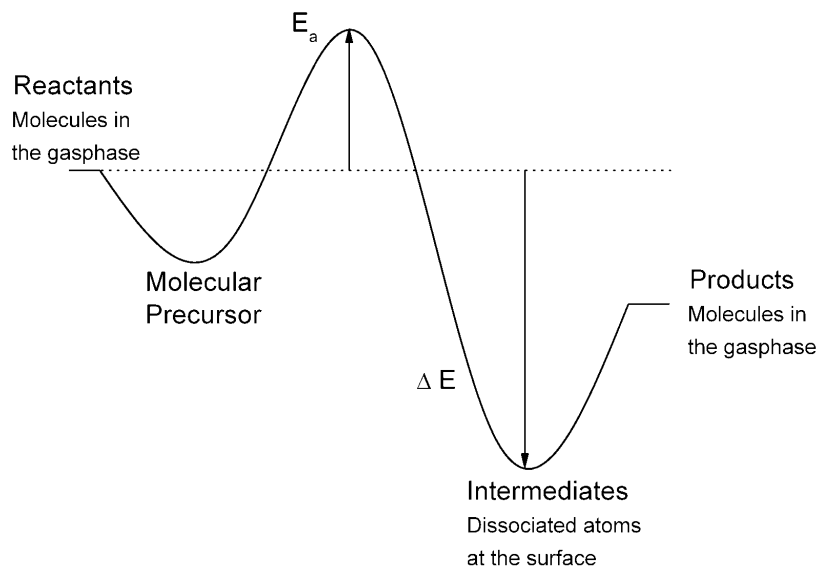


Fig. 1 Schematic energy diagram for a heterogeneously catalytic reaction.

When such a correlation appears, the trend in catalytic activity for metals of different reactivity in the periodic table can be understood directly based on a single descriptor, which we often choose to be the dissociative chemisorption energy of the key reactant. An activity trend such as the schematic plot shown in Fig. 2 will often appear (a volcano relation). For more reactive metals (ΔE further to the left), the removal of the dissociated reactants from the surface into the product gas phase will usually limit the catalytic rate. For the less reactive metals (to the right in Fig. 2), this desorption process is fast, and the dissociation barrier is high, so the catalytic rate is limited by the activation of the key reactants.

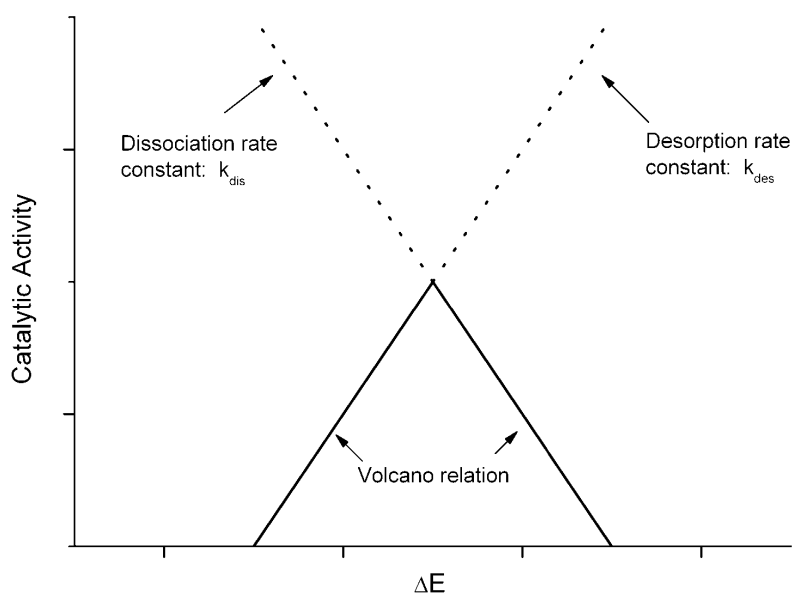


Fig. 2 Catalytic activity vs. the reaction energy of the dissociation reaction. More negative reaction energy (left) signifies that the adsorption reaction is more exothermic.

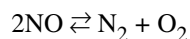
The optimal catalyst will be one having intermediate reaction energies, and the catalyst will be located at the top of the volcano curve. Sabatier realized this as early as 1911 [11].

DIRECT DECOMPOSITION OF NO OVER STEPPED TRANSITION-METAL SURFACES

The direct decomposition of NO is assumed to take place through four elementary reactions over a catalyst:

1. $\text{NO} + * \rightleftharpoons \text{NO}^*$
2. $\text{NO}^* + * \rightleftharpoons \text{N}^* + \text{O}^*$
3. $\text{N}^* + \text{N}^* \rightleftharpoons \text{N}_2 + 2*$
4. $\text{O}^* + \text{O}^* \rightleftharpoons \text{O}_2 + 2*$

A species denoted with an asterisk is adsorbed on an active site of the catalyst. An asterisk without a molecular or atomic species denotes a vacant active site on the surface. The full direct decomposition reaction is given by summing over the elementary reactions, and is given by



The decomposition reaction has two main parts: The first is the adsorption and dissociation of NO (elementary reactions 1 and 2), and the second part is recombination and the removal of N_2 and O_2 from the metal surface (elementary reactions 3 and 4).

In Fig. 3, images from the dissociation of NO on a stepped Rh surface are shown. The images show the initial, the transition, and the final state of the dissociation.

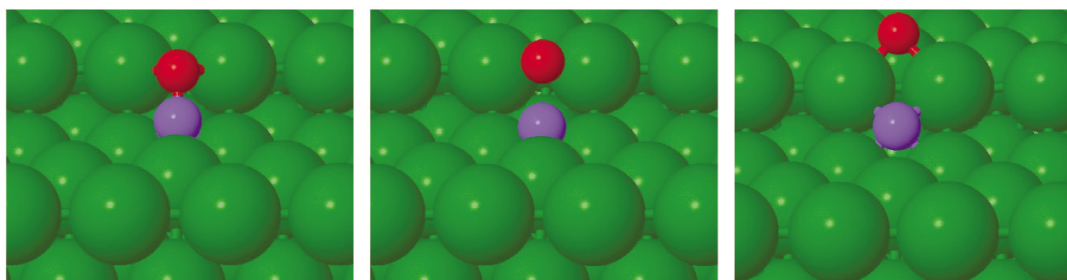


Fig. 3 Illustration of the dissociation of NO over a stepped (211) Rh surface as determined from DFT calculations. Left: initial state. Middle: transition state. Right: final state.

It has long been assumed that a linear relation between the activation energy and the reaction energy exists. Such relations are called Brønsted–Evans–Polanyi (BEP) relations [12–14]. For the key reactants and products in the direct decomposition of NO over transition-metal surfaces, such a relation indeed appears. In Fig. 4, the activation barriers for dissociation of NO, O₂, and N₂ over a range of transition metals are shown as a function of their respective dissociative chemisorption energies [6].

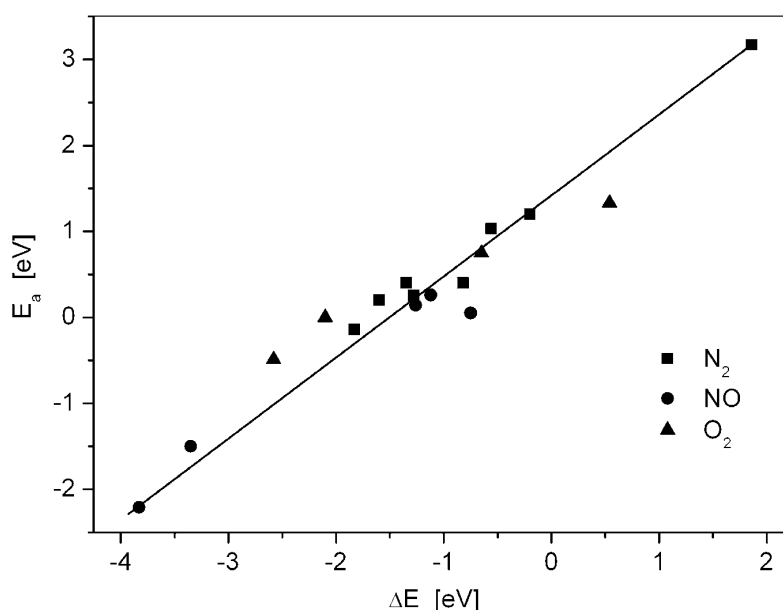


Fig. 4 “Universal” BEP relation for activation of diatomic molecules. (NO, N₂, and O₂). Adapted from ref. [6].

It appears that the correlation between transition states and dissociation energies is linear, and that the correlations for each of the diatomic molecules follow the same exact relationship. The relation also shows that the dissociation of NO will take place fast, when O and N are adsorbed strongly to the metal surface.

A good catalyst is a catalyst that lowers the activation barriers for each of the elementary reactions in the overall decomposition reaction. Therefore, according to Fig. 4, a good catalyst for the first part of the decomposition is a transition metal to which N and O adsorb strongly, since this will lower the activation barrier for dissociation of NO. The second part of the overall reaction is removal of N and O from the surface. This happens via associative desorption, elementary reactions 3 and 4. N₂ and O₂

associate at the surface and desorb immediately hereafter. This reaction is just the opposite of dissociative chemisorption and accordingly is favored by a weak adsorption of N and O. This rationale is what leads to the volcano curve in heterogeneous catalysis. Where the first part of the direct decomposition is favored by a strong adsorption of the reaction intermediates, the second part is favored by a weak adsorption. This suggests that intermediate surface reactivity will provide an optimal compromise and result in a fast overall rate.

When the correlation shown in Fig. 4 is combined with a set of adsorption energies on stepped transition- and noble-metal surfaces [15], a set of potential energy diagrams for the whole NO decomposition pathway over some of the most important stepped surfaces can be constructed. These energy diagrams are shown in Fig. 5. Of the pure transition- and noble-metal surfaces, it can be seen by inspection that the best catalysts must be Pt and Pd, since these do not over-bind intermediates to the same extent as Rh and Ru, while at the same time they do not present the same problems of unstable reaction intermediates on the surface as Ag and Au.

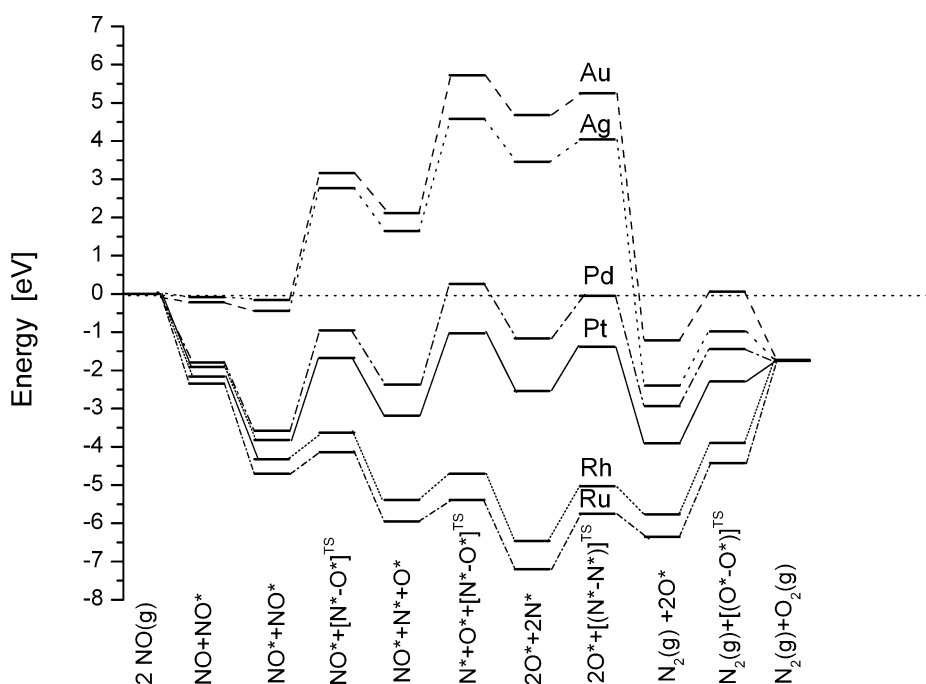


Fig. 5 Potential energy diagrams for the direct NO decomposition reaction over transition-metal surfaces.

WHICH CATALYST IS OPTIMAL? A DFT STUDY

In the previous section, we described the characteristics a catalyst must possess in order to decompose NO directly to N_2 and O_2 . We will now demonstrate how we are able to determine, by the use of DFT and microkinetic modeling, the rate on a more quantitative yet still analytical form [16]. The reaction energy for each elementary reaction was obtained using a plane-wave pseudopotential implementation of DFT. The publicly available program Dacapo [17] was employed. From the BEP relation shown in Fig. 4, we can obtain the activation barrier for each elementary reaction. For each elementary reaction, the rate has been obtained using the Sabatier–Gibbs model [18]. The temperature was 600 K, and the initial pressure of NO was 0.01 bar [16]. This model is particularly useful when looking at catalytic trends in systems which are inhibited by high coverages of some key intermediates. In the Sabatier–Gibbs analysis, we start from the assumption that the catalyst is running in the steady state,

meaning time-independent average mean-field coverages. It can be proven that the chemical potential of any species in the reaction is constrained to be in the interval between the chemical potentials defined by the equilibrium between that species and the reactants and the products, respectively. The boundaries on the chemical potential of each intermediate then yield boundaries on the coverage of all the different intermediates. The boundaries on the coverages yield boundaries on the catalytic rate, and the maximal possible rate obtainable under these constraints we refer to as the Sabatier–Gibbs rate. The Sabatier–Gibbs rate for the decomposition of NO to N_2 and O_2 , is then the minimum of the individual rates. In Fig. 6, the rates for the individual elementary reactions are shown together with the Sabatier–Gibbs rate.

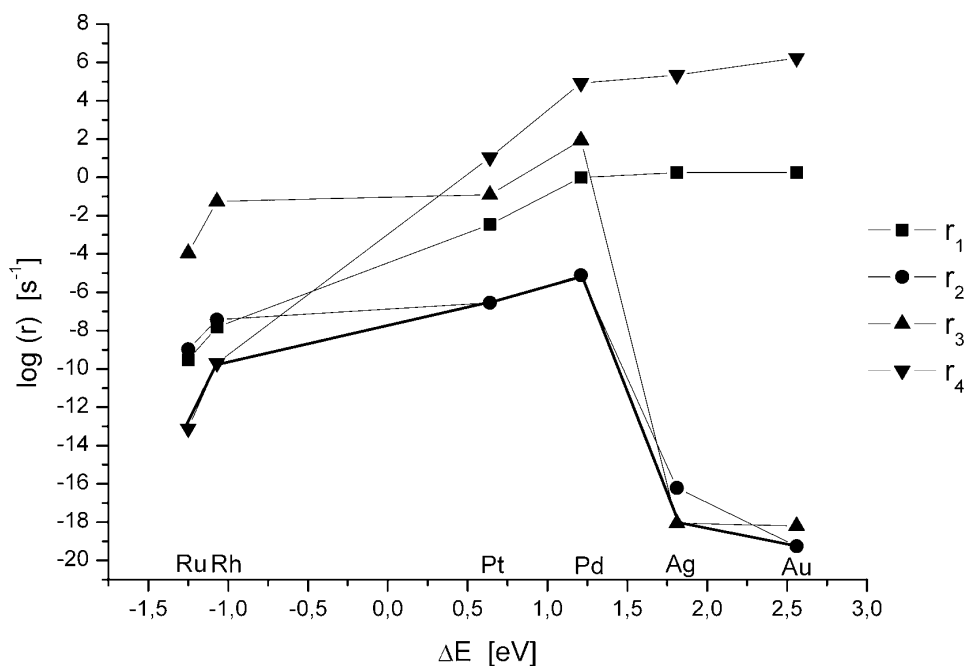


Fig. 6 Sabatier–Gibbs rates for each elementary reaction and the Sabatier–Gibbs volcano curve vs. the dissociation energy of adsorbed NO. Here, r_1 is the rate for adsorption of NO, r_2 is the rate for dissociation of NO, r_3 is the rate for associative desorption of N_2 , and r_4 is the rate for associative desorption of O_2 .

The first elementary reaction is adsorption of NO to the metal surface. The rate of this process is denoted r_1 . The model predicts that the adsorption is faster on the more noble metals such as, for example, Ag and Au, than on more reactive metals, such as Rh and Ru. The surfaces of the more reactive metals (Rh, Ru) will be entirely covered by oxygen due to the significant negative adsorption energy. Therefore, an extremely limited amount of free sites will be available for adsorption of NO. On the noble metals, the adsorption of O_2 is less facile, and many free sites are available for adsorption of NO on these surfaces. The next step is dissociation of NO. The dissociation is most activated on the more reactive metals, due to the stronger adsorption of the intermediates. However, as shown in Fig. 3, in order for the dissociation to take place free sites must be available for the atomic N and O. The dissociation rate is fastest on Pd and slowest on Au, which is in good agreement with the fact that Pd is more reactive than Au. The Rh surface is, however, so reactive that it will be covered with oxygen. Therefore, the amount of free sites is very limited, and this is the reason why the dissociation of NO is slower on Rh than, e.g., Pd. The two final steps is associative desorption of N and O from the metal to the gas phase. Intuitively, we know that a strong adsorption will limit the desorption rate. This is also what is

observed. The associative desorption of O_2 is slowest on Rh and fastest on Au. This is almost the same picture as for N_2 , however, N hardly adsorbs to Au and Ag, and therefore N will not be present. On Fig. 6, a volcano curve is highlighted. The volcano curve is constructed for each metal. It is seen that Pd is the most active metal for NO decomposition.

EXPERIMENTAL VERIFICATION

In order to show that the model correctly describes the catalytic activity of the transition metals in NO decomposition, a comparison between theoretically predicted rates and experimentally obtained results is shown in Fig. 7.

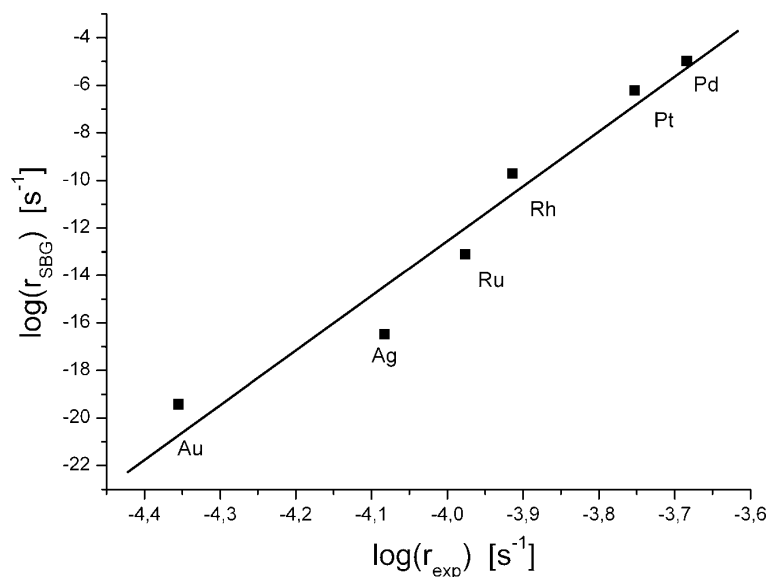


Fig. 7 Modeled decomposition rate vs. experimental results for a range of different transition-metal surfaces (obtained from ref. [16]).

The Sabatier–Gibbs rate is compared to experimental measurements of the direct NO decomposition reaction rates over various surfaces, and the qualitative agreement is striking, even if the absolute magnitude of the theoretically determined rates is less well determined.

In Fig. 8, the theoretically calculated direct NO decomposition rates are shown as a function of the dissociative chemisorption energies of N_2 and O_2 . A two-dimensional overall volcano is formed. It is interestingly observed that the transition metals lay on a line that is situated several eVs above the optimal point of the two-dimensional volcano. This indicates that one could find a much better transition-metal catalyst for direct NO decomposition, if only a metal could be chosen, which binds N atoms much strongly compared to O atoms. However, since the dissociative chemisorption energy for these species is linearly related, no such transition-metal catalyst can be found. This suggests that one needs to look into entirely different classes of materials in order to find appropriate direct NO decomposition catalysts, and that a more appropriate class of materials should have the property that N and O binds with a more equal strength to the surface.

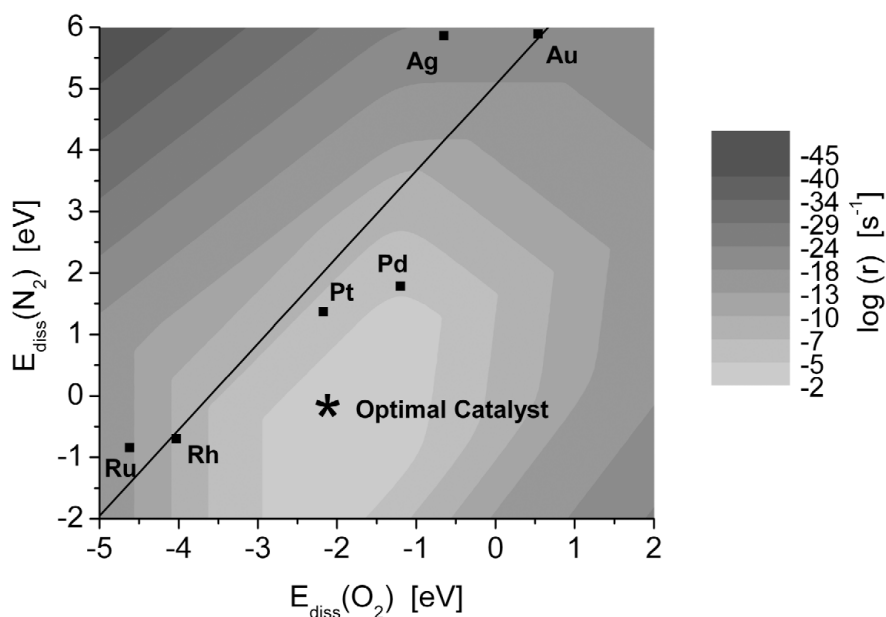


Fig. 8 Theoretically predicted decomposition rate as a function of the dissociative chemisorption energies of N_2 and O_2 . The dissociative chemisorption energies for N_2 and O_2 over a range of stepped transition-metal surfaces are also shown. The line represents the linear relation between the dissociative chemisorption energies for the transition metals.

CONCLUSION

The direct decomposition of NO on transition metals can be understood in detail from DFT studies. Linear correlations between reaction energies and activation barriers lead to clear trends, where Au and Ag have problems activating NO, while Rh and Ru rapidly becomes poisoned by strongly binding O atoms (especially on the most active step sites). Pd and Pt show the best catalytic activities among the pure metals treated in the present study, but the activity is still much too low in order for the pure metal surfaces to be useful direct NO decomposition catalysts for automotive purposes under lean-burn conditions. The model enables us to understand the volcano curve for decomposition of NO and thereby understand the trend in catalytic activity of the transition metals. Furthermore, the results are in good qualitative agreement with experimental results. The modeling clearly identifies one important underlying origin for the limited attainable catalytic activity of the stepped transition-metal surfaces with respect to direct NO decomposition, which is the too strong adsorption of O compared to N.

ACKNOWLEDGMENTS

The Center for Sustainable and Green Chemistry is funded by the Danish National Research Foundation, and the Center for Atomic-scale Materials Design is funded by the Lundbeck Foundation. We wish to acknowledge support from the Danish Research Agency through the framework program number 26-04-0047 and the Danish Center for Scientific Computing through grant HDW-0107-07.

REFERENCES

1. V. Smil. *Nature* **400**, 415 (1999).
2. H. Mahzoul, J. F. Brilhac, P. Gilot. *Appl. Catal., B* **20**, 47 (1999).
3. H. Burch, J. P. Breen, F. C. Meunier. *Appl. Catal., B* **39**, 283 (2002).
4. C. T. Goralski Jr., W. F. Schneider. *Appl. Catal., B* **37**, 263 (2002).
5. B. Hammer. *Phys. Rev. Lett.* **83**, 3681 (1999).
6. J. K. Nørskov, T. Bligaard, A. Logadottir, S. Bahn, L. B. Hansen, M. Bollinger, H. Benggaard, B. Hammer, S. Sljivancanin, M. Mavrikakis, Y. Xu, S. Dahl, C. J. H. Jacobsen. *J. Catal.* **209**, 275 (2002).
7. Q. Ge, M. Neurock. *J. Am. Chem. Soc.* **126**, 1551 (2004).
8. Z.-P. Liu, S. J. Jenkins, D. A. King. *J. Am. Chem. Soc.* **125**, 14660 (2003).
9. B. Hammer. *Top. Catal.* **37**, 3 (2006).
10. D. R. Rainer, S. M. Vesecky, M. Koranne, W. S. Oh, D. W. Goodman. *J. Catal.* **167**, 234 (1997).
11. P. Sabatier. *Ber. Dtsch. Chem. Ges.* **44**, 1911 (1984).
12. A. Logadottir, T. H. Rod, J. K. Nørskov, B. Hammer, S. Dahl, C. J. H. Jacobsen. *J. Catal.* **197**, 229 (2001).
13. N. Brønsted. *Chem. Rev.* **5**, 231 (1928).
14. M. G. Evans, M. Polanyi. *Trans. Faraday Soc.* **34**, 11 (1938).
15. T. Bligaard, J. K. Nørskov, S. Dahl, J. Matthiesen, C. H. Christensen, J. S. Sehested. *J. Catal.* **224**, 206 (2004).
16. H. Falsig, T. Bligaard, J. Rass-Hansen, A. L. Kustov, C. H. Christensen, J. K. Nørskov. *Top. Catal.* **45**, 117 (2007).
17. B. Hammer, L. B. Hansen, J. K. Nørskov. *Phys. Rev. B* **741**, 359 (1999).
18. T. Bligaard, H. Falsig, C. H. Christensen, J. K. Nørskov. "Sabatier-Gibbs Analysis of Microkinetic Models", in preparation.